BJP British Journal of Pharmacology

DOI:10.1111/bph.12076
www.brjpharmacol.org

RESEARCH PAPER

Citrus fruit and fabacea secondary metabolites potently and selectively block TRPM3

I Straub[1], F Mohr[2], J Stab[2], M Konrad[2], SE Philipp[3], J Oberwinkler[2] and M Schaefer[1]

[1]*Rudolf-Boehm-Institut für Pharmakologie und Toxikologie, Universität Leipzig, Leipzig, Germany,* [2]*Institut für Physiologie und Pathophysiologie, Philipps-Universität Marburg, Marburg, Germany, and* [3]*Experimentelle und Klinische Pharmakologie und Toxikologie, Universität des Saarlandes, Homburg, Germany*

Correspondence
M Schaefer,
Rudolf-Boehm-Institut für Pharmakologie und Toxikologie, Universität Leipzig, Härtelstr. 16-18, 04107 Leipzig, Germany.
E-mail: michael.schaefer@medizin.uni-leipzig.de

Keywords
TRP channels; flavonoids; DRG neurones

Received
5 July 2012
Revised
6 November 2012
Accepted
19 November 2012

BACKGROUND AND PURPOSE

The melastatin-related transient receptor potential TRPM3 is a calcium-permeable nonselective cation channel that can be activated by the neurosteroid pregnenolone sulphate (PregS) and heat. TRPM3-deficient mice show an impaired perception of noxious heat. Hence, drugs inhibiting TRPM3 possibly get in focus of analgesic therapy.

EXPERIMENTAL APPROACH

Fluorometric methods were used to identify novel TRPM3-blocking compounds and to characterize their potency and selectivity to block TRPM3 but not other sensory TRP channels. Biophysical properties of the block were assessed using electrophysiological methods. Single cell calcium measurements confirmed the block of endogenously expressed TRPM3 channels in rat and mouse dorsal root ganglion (DRG) neurones.

KEY RESULTS

By screening a compound library, we identified three natural compounds as potent blockers of TRPM3. Naringenin and hesperetin belong to the citrus fruit flavanones, and ononetin is a deoxybenzoin. Eriodictyol, a metabolite of naringenin and hesperetin, was still biologically active as a TRPM3 blocker. The compounds exhibited a marked specificity for recombinant TRPM3 and blocked PregS-induced $[Ca^{2+}]_i$ signals in freshly isolated DRG neurones.

CONCLUSION AND IMPLICATIONS

The data indicate that citrus fruit flavonoids are potent and selective blockers of TRPM3. Their potencies ranged from upper nanomolar to lower micromolar concentrations. Since physiological functions of TRPM3 channels are still poorly defined, the development and validation of potent and selective blockers is expected to contribute to clarifying the role of TRPM3 *in vivo*. Considering the involvement of TRPM3 in nociception, TRPM3 blockers may represent a novel concept for analgesic treatment.

Abbreviations

$[Ca^{2+}]_i$, intracellular free Ca^{2+} concentration; DRG, dorsal root ganglion; HBS, HEPES-buffered solution; NSAIDs, non-steroidal anti-inflammatory drug; PregS, pregnenolone sulphate; TRPA, transient receptor potential ankyrin-like; TRPM, transient receptor potential melastatin-related; TRPV, transient receptor potential vanilloid-related

Introduction

TRPM3, the third member of the melastatin-related TRPM channel subfamily, is still poorly characterized. The TRPM3 gene is transcribed into different alternative splice variants. Alternative splicing in a region that encodes the putative pore region of TRPM3 changes the selectivity of ion permeation. Whereas the TRPM3α2 variant is a calcium-permeable, poorly selective cation channel, TRPM3α1 features 12 additional amino acids within the pore domain and is selective for monovalent cations (Oberwinkler *et al.*, 2005). In this manuscript, we focus on the TRPM3α2 variant, which is expressed in various neuronal and non-neuronal tissues and can be activated by the neurosteroid pregnenolone sulphate (PregS) or high concentrations of nifedipine (Wagner *et al.*, 2008), by noxious heat (Vriens *et al.*, 2011), and by D-erythro-sphingosine (Grimm *et al.*, 2005).

The physiological role of TRPM3 is still not firmly established. PregS-induced activation of TRPM3 has been linked to insulin secretion in pancreatic beta-cells (Wagner *et al.*, 2008), to vascular smooth muscle cell contraction (Naylor *et al.*, 2010), and to potentiation of glutamatergic transmission in cerbellar Purkinje neurons from developing rats (Zamudio-Bulcock *et al.*, 2011). Recently, Vriens *et al.* observed that TRPM3-deficient mice show an impaired perception of noxious heat. Hence, drugs inhibiting TRPM3 may provide novel instruments for analgesic therapy. In addition, TRPM3 blockers may help to unravel biological functions of TRPM3 that might be obscured by compensatory effects in gene targeting or knock-down approaches.

TRPM3 channel blockers described so far include the antidiabetic PPARγ-agonists rosiglitazone and troglitazone (Majeed *et al.*, 2011) and nonsteroidal anti-inflammatory drugs (NSAIDs) of the fenamate group (Klose *et al.*, 2011). Furthermore, TRPM3 is blocked by 2-APB (Xu *et al.*, 2005) or by lanthanum and gadolinium ions (Harteneck and Schultz, 2007) that block a plethora of different TRP channels.

By screening a compound library, we identified three natural compounds as potent TRPM3 blockers. Two of them, naringenin and hesperetin, belong to the citrus fruit flavanones and ononetin is a deoxybenzoin. Based on its structural similarity to naringenin and hesperetin, we also identified eriodictyol as a potent TRPM3 blocker. Furthermore, we confirm the biological activity of naringenin, ononetin and eriodictyol in natively TRPM3-expressing dorsal root ganglia (DRG) neurones.

Methods

Cell culture

HEK293 cells used for transient transfection with TRPM1 were cultured in MEM medium (Invitrogen, Darmstadt, Germany) containing 10% FCS at 37°C and 5% CO_2. Cells were passaged one to three times a week. HEK293 cells were cultured in Earle's Minimum Essential Medium supplemented with 10% fetal calf serum, 2 mM L-glutamine, 100 units·mL^{-1} penicillin, 0.1 mg·mL^{-1} streptomycin. For generation of a HEK293 cell line stably expressing myc-tagged mouse TRPM3α2 (HEK_{mTRPM3}), the cDNA of the myc epitope was introduced in frame after the start codon of the TRPM3α2 cDNA (GenBank accession AJ544535), ligated into pcDNA3 and transfected into HEK293 cells. Transfected cells were selected in a medium containing 500 μg·mL^{-1} G418 for 4 weeks. Single cells were separated by FACS on a MoFlo cell sorter (Beckmann Coulter, Krefeld, Germany) and expanded. Clones were tested in Western blots using monoclonal anti-TRPM3 and anti-myc antibodies, and analysed for PregS-induced Ca^{2+} signals in single cell calcium measurement experiments. HEK293 cells stably expressing other sensory TRP channels (HEK_{hTRPA1}, $HEK_{hTRPM8:CFP}$, $HEK_{rTRPV1:YFP}$) were obtained by a limiting dilution method as described recently (Hellwig *et al.*, 2004; Urban *et al.*, 2012). All cells were grown at 37°C in a humidified atmosphere containing 5% CO_2. Unless otherwise stated, cells were seeded 24 h prior to the experiments on poly-L-lysine-coated coverslips.

DRG neuron preparation

Adult C57BL6/N mice, bred and kept at the local animal care facility (Uniklinikum des Saarlandes, Homburg, Germany) were killed by an overdose of i.p. urethane (25% in 0.9% NaCl solution). Mice were opened from the dorsal side, and the spinal cord was carefully exposed. The spinal cord was then gently removed; and DRG from all cervical, thoracic and lumbar segments were obtained. Ganglia were digested for 15 min at 37°C in an enzyme solution containing 0.1 mg·mL^{-1} trypsin (Sigma-Aldrich, Deisenhofen, Germany), and 44.4 μg·mL^{-1} liberase DH (Roche, Mannheim, Germany), dissolved DMEM in (Gibco; Invitrogen). After repeated trituration with a 1 mL pipette, the digestion was stopped by adding 100 μL FCS; the cell suspension was centrifuged (3.5 min at 670 g) and resuspended in DMEM medium, supplemented with 10% FCS, 100 units·mL^{-1} penicillin, and 0.1 mg·mL^{-1} streptomycin. Subsequently, droplets of cell suspension were plated on poly-D-lysine (1 mg·mL^{-1}; Sigma-Aldrich)-coated coverslips, placed in a culture dish and left to adhere for at least 1 h in an incubator (37°C, 5% CO_2). The culture dish was then filled with growth medium. All experiments were performed within 36 h after preparation.

To obtain rat DRG neurones, 8 week-old Wistar rats were killed by an overdose of CO_2. The preparation of DRG neurones was performed as described above. For patch clamp measurements, NGF (30 ng·mL^{-1}; Sigma-Aldrich) was added to the medium. Wistar rats (Janvier, Saint Berthevin Cedex, France) were housed under a 12 h light–dark cycle and allowed access to laboratory animal feed and water *ad libitum*. All studies involving animals are reported in accordance with the ARRIVE guidelines for reporting experiments involving animals (Kilkenny *et al.*, 2010; McGrath *et al.*, 2010). All experimental procedures involving animals were approved by the Committee on Animal Care and Use of the local governmental body. Procedures were optimized to reduce the number of animals and their suffering, according to the regulations of the German Animal Welfare Act. A total number of nine animals (two mice and seven rats) were used in experiments described here.

Cell transfection

HEK293 cells were transiently transfected with a bi-cistronic plasmid encoding Myc-tagged TRPM1 and enhanced green fluorescent protein as previously described (Lambert *et al.*,

2011). The Polyfect transfection reagent (Qiagen, Hilden, Germany) was used according to the instructions of the manufacturer. One day after the transfection, cells were split and reseeded at a reduced density. Cells were used for experiments 36 to 72 h after the transfection. For heat activation of TRPM3, HEK293 cells were transiently transfected with a plasmid encoding TRPM3α2-GFP. Transfection was performed with FugeneHD (Promega, Mannheim, Germany) and 48 h after transfection, cells were split and reseeded on poly-L-lysine-coated coverslips.

Intracellular Ca^{2+} analysis in cell suspensions

All fluorometric assays in cell suspensions were performed at room temperature in a 384-well microtitre plate format. For detailed information, see Norenberg *et al.* (2011). Shortly, HEK293 cells stably expressing TRPM3 were incubated with Fluo-4/AM (4 μM; Molecular Probes, Invitrogen) for 30 min at 37°C, washed and resuspended in HEPES-buffered solution (HBS) buffer, containing 135 mM NaCl, 6 mM KCl, 1 mM $CaCl_2$, 1 mM $MgCl_2$, 5.5 mM D-glucose, and 10 mM HEPES adjusted to pH 7.4 with NaOH. For the primary screening, wells were prefilled with individual compounds of a Spectrum Collection compound library (MicroSource Discovery Systems, Gaylordsville, CT) at a final concentration of 20 μM. Measurement was executed with a filter-based plate reader device (Polastar Omega, BMG Labtech, Offenburg, Germany), applying 485/10- and 520/20-nm band pass filters. After recording a baseline of 160 s (10 cycles), PregS 35 μM, final concentration, was injected into each well; and fluorescence intensities were followed for 10 min after agonist injection. To obtain concentration–response functions, various concentrations of the blocking compounds were pre-incubated for 10–15 min, and data were subjected to nonlinear curve fitting applying a four-parameter Hill equation (E_{min}, E_{max}, IC_{50} and Hill coefficient).

Measurements of agonistic properties of the compounds were performed using a custom-made fluorescence plate imaging device built into a robotic liquid handling station (Freedom Evo 150, Tecan, Switzerland). The plate imaging device comprised a 460-nm LED array, filtered with a 475 nm short-pass filter (DT-blue, Optic Balzers, Oerlikon, Switzerland) and a cooled CCD camera (Coolsnap FX, Photometrics, Tucson, AZ), equipped with a Xenon 0.95/25 C-mount lens (Schneider Kreuznach, Bad Kreuznach, Germany), and a 515 nm long-pass filter (Y515-Di, Fujifilm, Tokyo, Japan). The imaging was controlled with the MicroManager software (Edelstein *et al.*, 2010), and fluorescence intensities were quantified over single wells, corrected for background signals and expressed as F/F_0, using ImageJ (Abramoff *et al.*, 2004).

Single-cell calcium measurement

Transfected HEK293 cells attached to coverslips were loaded with 5 μM Fura-2/AM (Biotium, Hayward, CA, USA) for 30 min at room temperature or, in the case of DRG neurons, at 37°C. Coverslips were mounted in a recording chamber (Warner Instruments, Hamden, CT, USA) and superfused with the aid of a computer-controlled valve bench (ALA Scientific, Farmingdale, NY, USA). For the measurements in mouse DRG neurones, we used the same extracellular solution as for whole-cell patch clamp measurements (see below). For measurement of transfected HEK293 cells, the bath solution contained 3 mM glucose and 7 mM mannitol instead of 10 mM glucose. Images were captured at alternating excitation wavelengths of 340 and 380 nm with a 10× SFluor objective (Nikon, Düsseldorf, Germany) and a cooled CCD camera (QImaging, Surrey, Canada). Background subtraction and ratio calculation were performed with ImageJ utilizing a modified version of the 'ratio-plus' plugin.

For single-cell $[Ca^{2+}]_i$ measurement in rat DRG neurones, coverslips were mounted on a monochromator-equipped (Polychrome, TILL-Photonic) inverted epifluorescence microscope (Carl Zeiss, Jena; 10×/0.5 Fluar objective), and superfused with HBS buffer. Detection and calibration of the calcium concentration was performed with a spectral unmixing method as described earlier (Lenz *et al.*, 2002). All measurements were performed at room temperature.

Whole-cell patch clamp measurements

Standard electrophysiology methods were used. All measurements were performed at room temperature, expect for temperature activation of TRPM3, using an Axopatch 200B amplifier with a Digidata 1200 digitizer (Axon CNS, Molecular Devices, Sunnyvale, CA, USA) under the control of the Pclamp 9 software (Molecular Devices). Voltage ramps (from –113 to +87 mV, 1 $mV \cdot ms^{-1}$) were applied every second from a holding potential of –13 mV. The intracellular solution contained 80 mM Cs-aspartate, 45 mM CsCl, 4 mM Na_2ATP or $TRIS_2$-ATP, 10 mM HEPES, 10 mM BAPTA, pH 7.2 adjusted with CsOH. The osmolarity was 300–315 mosm. The extracellular solution used contained 145 mM NaCl, 3 mM KCl, 10 mM CsCl, 2 mM $CaCl_2$, 2 mM $MgCl_2$, 10 mM HEPES, 10 mM D-glucose, pH 7.4 adjusted with NaOH. The liquid junction potential of approximately 13 mV between the bath solution and the pipette solution (calculated with Clampex, Axon Instruments, Molecular Devices) was corrected. The sampling rate was 5 kHz in standard whole-cell measurements. During fast application of naringenin, the sampling rate was 20 kHz. Modulators were applied via a SF-77B Perfusion Fast Step system (Warner Instruments). Current decay kinetics were calculated with Clampfit 9.2 (Molecular Devices), using a biexponential fitting. For heat activation of TRPM3, the bath solution was cooled to 17–20°C under control conditions. To activate and block TRPM3, pre-cooled solutions were heated to 37–40°C with an inline solution heater (Warner Instruments) under control of a TC-324B Temperature Controller (Warner Instruments). To monitor the actual temperature of the bath solution, a thermistor electrode was situated in the vicinity of the patched cell, and the temperature was logged during the measurement with the Pclamp 9 software. For recordings in DRG neurones, the extracellular solution contained 140 mM NaCl, 2 mM $MgCl_2$, 4 mM KCl, 0.5 mM lidocain, 10 mM TRIS (pH 7.4 with HCl), and the pipette solution contained 140 mM CsCl, 0.6 mM $MgCl_2$, 1 mM EGTA, 10 mM HEPES, 5 mM TEA (pH 7.2 with CsOH). Although lidocain activates recombinant rTRPV1 with an EC_{50} of about 12 mM (Leffler *et al.*, 2008), the concentration we used to block voltage-dependent sodium channels should not strongly influence TRPV1.

Stock solutions and drugs

All modulators were dissolved in DMSO. The concentration of stock solutions was chosen in such a way that the DMSO

concentration in the final solution never exceeded 0.14% at the highest concentration of the respective modulator and further reduced by serial dilution of the compounds. PregS, naringenin, hesperetin, eriodictyol and ononetin were purchased from Sigma-Aldrich.

Statistical analysis

All error bars represent the SEM. The number of cells analysed in each experiment is indicated in the figure legends. To test for statistically significant differences, we used ANOVA with the Tukey's post test. In the figures, one star indicates $P < 0.05$, two stars indicate $P < 0.01$, three stars indicate $P < 0.001$.

Results

Screening for compounds that modulate TRPM3 channel activity

To identify compounds that exert a biological activity to modulate TRPM3, we performed a medium throughput screen. To this end, the Spectrum Collection compound library, comprising 2000 drugs, drug-like molecules, natural compounds or toxins, was used at a final concentration of 20 μM. HEK293 cells stably expressing mTRPM3 (HEK_{mTRPM3}) were loaded with the fluorescent calcium indicator dye Fluo-4, dispensed into 384-well plates, and PregS-induced calcium entry was detected. As a result of the primary screen, we identified three compounds that completely blocked the PregS-induced calcium entry (Figure 1A–C). Furthermore, we confirmed the previously identified TRPM3 channel-blocking properties of the fenamates tolfenamic acid and mefenamic acid (Klose *et al.*, 2011). The three newly identified blocking compounds belong to a class of plant secondary metabolites. The flavonoids naringenin and hesperetin are contained in grapefruits and oranges respectively. Ononetin is a deoxybenzoin that has originally been synthesized from *Ononis spinosa*-derived isoflavanones, but may also be obtained from fabaceae. In grapefruit, a major fraction of naringenin is conjugated with the disaccharide neohesperidose. This glycoside is referred to as naringin, and accounts for the bitter taste of grapefruit (Manach *et al.*, 2004). Interestingly, neither naringin nor hesperidin, the glycoside of hesperetin, blocked TRPM3 (Figure 1A,B).

Hit verification in a secondary screen with freshly dissolved compounds confirmed the ability of the citrus fruit flavanones and ononetin to block TRPM3. Furthermore, we found that eriodictyol, which is found in lemons or formed by hepatic metabolism of naringenin and hesperetin (Breinholt *et al.*, 2002), completely blocked the PregS-induced Ca^{2+} entry in HEK_{mTRPM3} cells when pre-incubated at a concentration of 20 μM (Figure 1D,E).

Concentration dependence and electrophysiological properties of the flavonoid-induced TRPM3 block

To evaluate the potency of the flavonoids to block TRPM3, we used a fluorometric Ca^{2+} assay to obtain concentration-response curves. HEK_{mTRPM3} cells were incubated with different concentrations of the test compounds, and PregS-induced calcium entry was measured. The applied PregS concentration of 35 μM is higher than the reported EC_{50} of 12 and 23 μM for TRPM3 inward and outward currents (Wagner *et al.*, 2008) but is not yet saturating. Naringenin and hesperetin displayed a potent block with IC_{50} values of 0.5 ± 0.07 μM (Figure 2A) and 2.0 ± 0.1 μM (Figure 2B) respectively. Ononetin displayed an IC_{50} of 0.3 ± 0.03 μM (Figure 2C) and eriodictyol blocked TRPM3 with an IC_{50} of 1.0 ± 0.07 μM (Figure 2D). The Hill coefficients ranged between 1.4 and 2.2 for the investigated compounds (see Figure 2).

To further characterize the new blockers, we performed whole-cell patch clamp measurements in the presence of naringenin (Figure 3) and ononetin (Figure 4). The onset of the naringenin-induced block was fast, but a complete block was only achieved after a few seconds (Figure 3A). Wash-out of naringenin allowed a reactivation of TRPM3 channels with PregS (Figure 3A). However, naringenin-blocked TRPM3 currents recovered only slowly after removal of the modulator (Figure 3A). Applying I/V ramp protocols, we observed that the naringenin-induced block is largely voltage-independent (Figure 3B) and reversible. In order to more rapidly deliver the compound to the patched cell, we performed some experiments with a fast application system and supramaximally effective concentrations of naringenin (Figure 3C). A biexponential fit of the decaying current kinetic revealed fast and slow τ-values of 291 and 2370 ms. The major component of the current (77%) decayed with τ_{fast}, and only 23% of the current was blocked with a τ_{slow} (Figure 3C). Interestingly, naringenin exerted a slightly higher blocking potency in whole-cell measurements compared with the calcium assay. Electrophysiologically measured concentration–response curves of naringenin showed that inward currents were more potently blocked (IC_{50} = 0.27 ± 0.04 μM) compared to the outward currents (IC_{50} = 0.37 ± 0.005 μM). Although the potency of TRPM3 block displayed some voltage dependence, both current components were naringenin-sensitive and almost completely blocked at a concentration of 3 μM (Figure S1).

The current decay after ononetin-induced block developed faster than the naringenin induced block of TRPM3, and the block was rapidly reversible (Figure 4A). Comparable to naringenin, ononetin blocked TRPM3 in a voltage-independent fashion (Figure 4B). In electrophysiological recordings, ononetin showed approximately the same efficiency as previously found in Fluo-4 measurements. A concentration of 0.3 μM ononetin blocked 62% ± 4% of PregS-induced currents at –113 mV and 53% ± 4% at +87 mV, and at a concentration of 3 μM, the currents were completely abolished (Figure 4C).

To exclude that the blocking effect of naringenin and ononetin is restricted to PregS activation of TRPM3, we performed whole-cell measurements with nifedipine as activator of TRPM3 (Wagner *et al.*, 2008). As shown in supplemental Figure 2, nifedipine (50 μM)-induced TRPM3 currents were concentration-dependently (tested concentrations: 1 μM and 3 μM) blocked by naringenin or ononetin.

Since heat may be a physiological activator of TRPM3, we tested if the newly identified compounds also block heat-induced TRPM3 currents. HEK293 cells transiently transfected with TRPM3α2 showed small outward and inward currents after raising the bath solution to temperatures above 37°C (Figure 5). These currents were partially blocked by

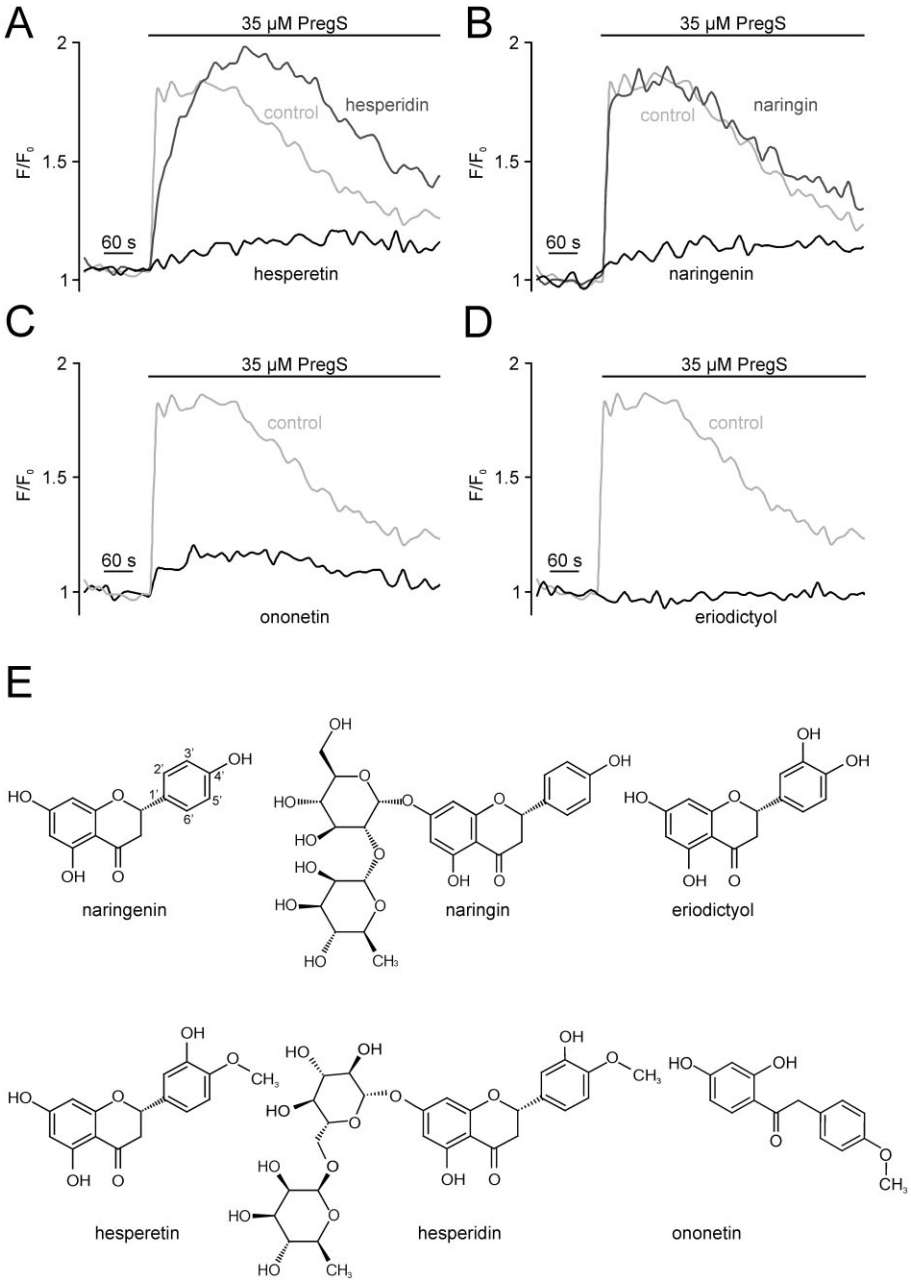

Figure 1

Identification of TRPM3 channel-blocking compounds. Fluo4-loaded HEK293 cells stably expressing TRPM3 (HEK_{mTRPM3}) were incubated with single compounds (20 µM) of the Spectrum Collection, and fluorescence intensities were detected during injection of the TRPM3 activator PregS. (A–D) Examples of calcium entry traces extracted from a single 384-well plate measurement. Light grey trace represents a DMSO control (A–D). Black trace: (A) hesperetin, (B) naringenin, (C) ononetin and (D) eriodictyol. Dark grey: (A) hesperidin and (B) naringin. (E) Chemical structures of verified hits naringenin, hesperetin, ononetin and eriodictyol as well as the flavonoid glycoside hesperedin and naringin.

5 µM naringenin and ononetin (Figure 5A). About 80% of the heat-dependent outward currents were blocked by naringenin or ononetin, whereas only 40–60% of the inward currents were blocked (Figure 5C). Hesperetin (10 µM) and eriodictyol (20 µM) also partially blocked heat-induced activation of TRPM3 (Figure 5D,E). Of note, raising the temperature in measurements with untransfected parental HEK cells also gave rise to substantial inward and outward currents (Figure 5F), In contrast to transfected HEK293 cells, ononetin and naringenin did not diminish neither inward nor outward currents in the untransfected parental HEK293 cells. We conclude that background currents that are not sensitive to TRPM3 blockers may cause an underestimation of the efficiency of blocker effects on the heat-activated TRPM3.

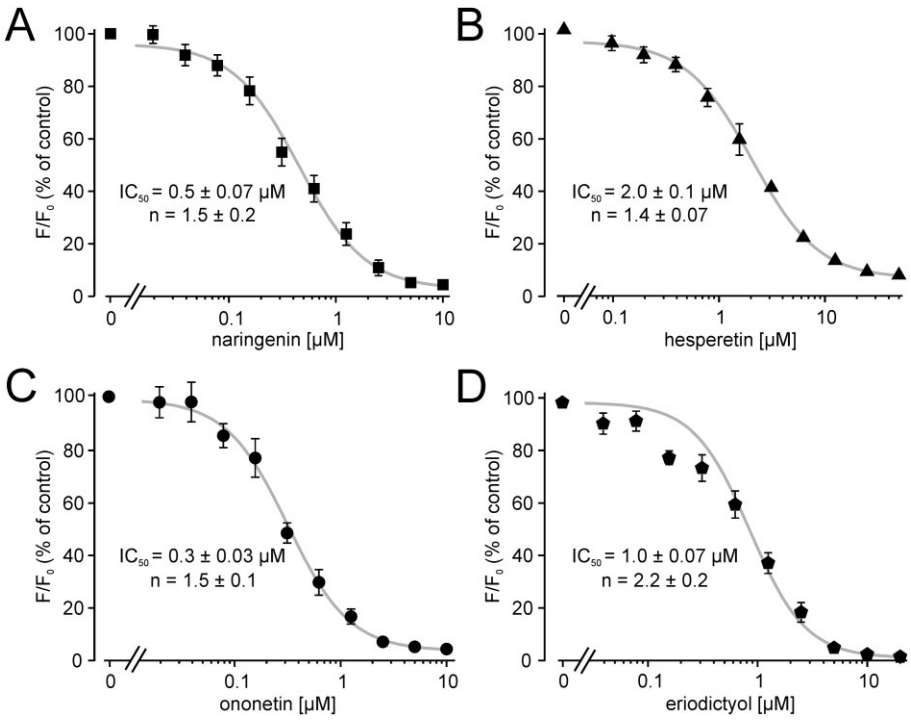

Figure 2

Concentration–response curves of TRPM3-blocking compounds. HEK_{mTRPM3} cell suspensions were incubated with various inhibitor concentrations as indicated. Fluorescence intensities were measured during PregS-induced activation of TRPM3. TRPM3 activation without an inhibitor was set as 100% and fluorescence intensities containing inhibitors were normalized to this value. (A–D) Concentration–response curves of naringenin, ononetin, hesperetin and eriodictyol are shown. Each data point represents at least six independent experiments for naringenin and ononetin and four independent experiments for hesperetin and eriodictyol with duplicates each. Shown are mean values and SEM. IC_{50} values and Hill coefficients (*n*) were obtained by non-linear curve fitting, applying a four-parameter Hill equation.

Biophysical properties of TRPM3 block by naringenin and ononetin

To more precisely specify the blocking mechanism we tested from which side of the plasma membrane naringenin and ononetin act on TRPM3 channels by adding the substances to the intracellular solution. Even at a concentration of 3 µM, intracellularly applied ononetin was unable to block PregS-induced currents in HEK_{mTRPM3} cells, whereas addition of the TRPM3 blocker to the bath solution was still effective (Figure 6A). Naringenin showed similar results, however at concentrations above 0.6 µM in the pipette, gigaseals were frequently lost during whole-cell patch-clamp measurements (Figure 6D). Although this concentration is sufficient to almost completely block PregS-induced currents when added from the outside (Figure 3C), there was no overt decrease in the current densities after PregS-induced TRPM3 channel activation in cells that were patched with naringenin in the pipette solution. These findings strongly hint at an extracellularly accessible binding site for naringenin and ononetin.

Electrophysiological measurements showed differences in the blocking behaviour of naringenin and ononetin. Whereas ononetin showed a fast and rapidly reversible block, the naringenin-induced block recovered with a slower off-rate. Together with the fact that PregS is an activator of TRPM3 channels from the extracellular side (Wagner *et al.*, 2008), these observations prompted us to investigate whether the blockers may interfere with the activator binding. To this end, TRPM3-expressing cells were incubated with naringenin or ononetin, and calcium entry was measured after activation of TRPM3 with different PregS concentrations (Figure 7). Lowering the PregS concentration did not lead to significant changes of the IC_{50} values of ononetin and naringenin. Increasing the concentration of PregS to 100 µM, however, shifted the IC_{50} of ononetin to a higher concentration (1.9 µM) (Figure 7A); whereas the IC_{50} of naringenin remained almost unaffected (Figure 7B).

Specificity of TRPM3 channel blockers

To examine the specificity of the blockers, we first investigated the ability of naringenin and ononetin to block the most closely related channel TRPM1. Like TRPM3, TRPM1 can be activated by PregS (Lambert *et al.*, 2011). At a concentration of 10 µM, naringenin did not exert a strong inhibition of the PregS-mediated calcium entry in HEK293 cells that express TRPM1 (Figure 8A). In contrast to naringenin, 10 µM ononetin partially attenuated the PregS-induced calcium responses in TRPM1-expressing cells by about 50% (Figure 8B). In agreement with Lambert *et al.*, TRPM1 channels were almost completely and reversibly blocked by 100 µM Zn^{2+} in contrast to TRPM3 channels (Wagner *et al.*, 2010).

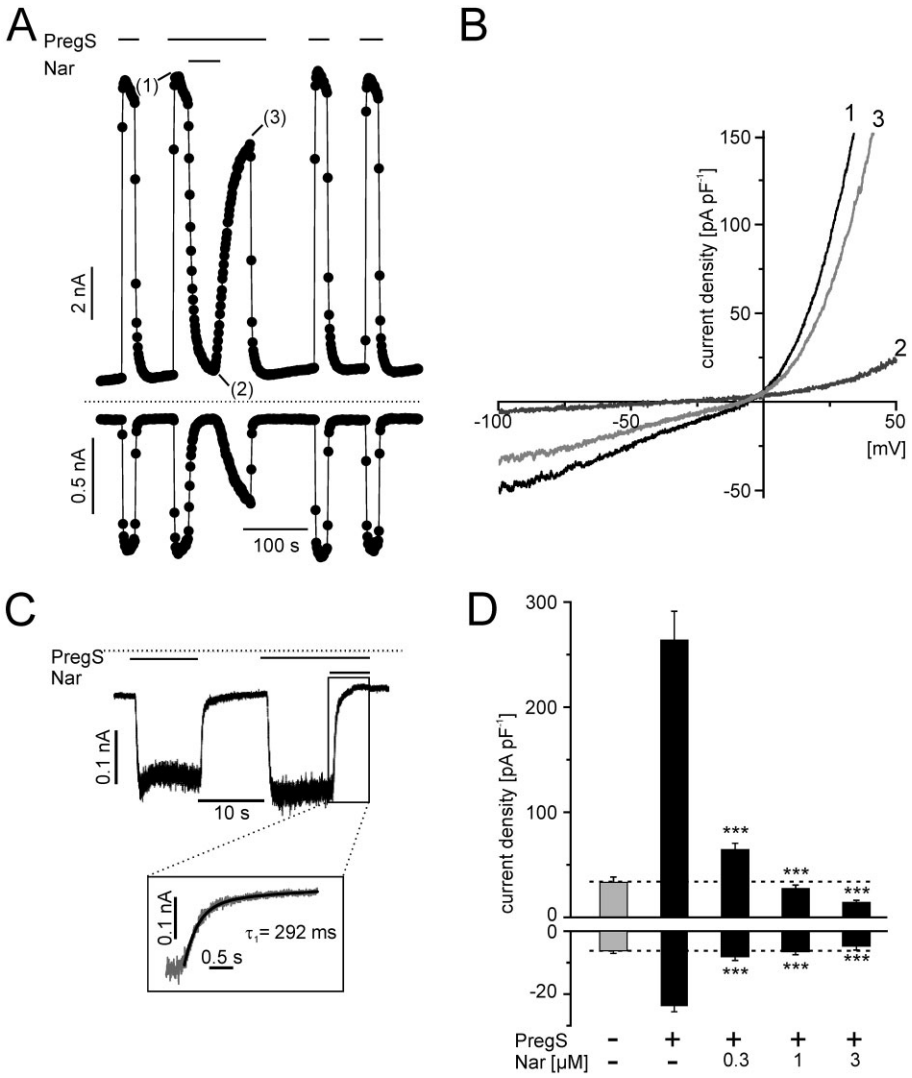

Figure 3

Electrophysiological properties of naringenin-mediated TRPM3 block. (A) Representative recordings of whole-cell currents in HEK_{mTRPM3} cells induced by 35 μM PregS and reversibly blocked with 3 μM naringenin. Data are extracted from voltage ramps and depict the current at 87 mV (upper trace) and –113 mV (lower trace). Dotted line: zero current level. (B) To assess the blocker activity in HEK_{mTRPM3} at different potentials, slow ramps (1 mV·ms^{-1}) ranging from –100 to 50 mV were applied in the presence of PregS before (1), during (2) and after (3) addition of 3 μM naringenin. (C) Representative whole-cell recording, a HEK_{mTRPM3} cell clamped at –83 mV, showing currents in response to 35 μM PregS and currents blocked with 10 μM naringenin. Naringenin was acutely applied with a fast perfusion system. Insert: superposition of the decaying phase of TRPM3 currents and a biexponential fit of the data. (D) Statistical analysis of 6–12 independent experiments performed as shown in (A), but with various concentrations of naringenin. Dashed line: Level of background conductivity in the absence of PregS and naringenin. Statistically significant differences of TRPM3 activation with PregS and block with naringenin are indicated as asterisks.

Since an involvement of TRPM3 in thermal nociception has been shown, we further investigated the ability of the flavanones hesperetin, naringenin and eriodictyol as well as the deoxybenzoin ononetin to block sensory TRP channels that are expressed in DRG neurones, including TRPA1, TRPM8 and TRPV1. Naringenin did not have an influence on TRPA1, whereas at very high concentrations, naringenin exerted a partial inhibition of TRPV1 (Figure 9A). Naringenin activated TRPM8 (Figure 9E) and prevented a subsequent activation by menthol (Figure S3A). Interestingly, menthol-induced currents in HEK cells expressing TRPM8 were blocked after an additional perfusion of the cells with naringenin (Figure S3B). However, further investigations are needed to clarify the complex mechanism of naringenin to block and activate TRPM8.

Hesperetin and eriodictyol neither blocked nor activated any tested TRP ion channels other than TRPM3 when applied in concentrations up to 50 μM (Figure 9B,D). Ononetin, the most potent TRPM3 channel blocker, activated TRPA1 in fluorometric measurements (Figure 9F) but had no overt influence on TRPM8 or TRPV1 at concentrations up to 100 μM (Figure 9C). Since many compounds that promote TRPA1 activation in fluorometric Ca^{2+} assays act in a light-dependent fashion (Hill and Schaefer, 2009), we reassessed

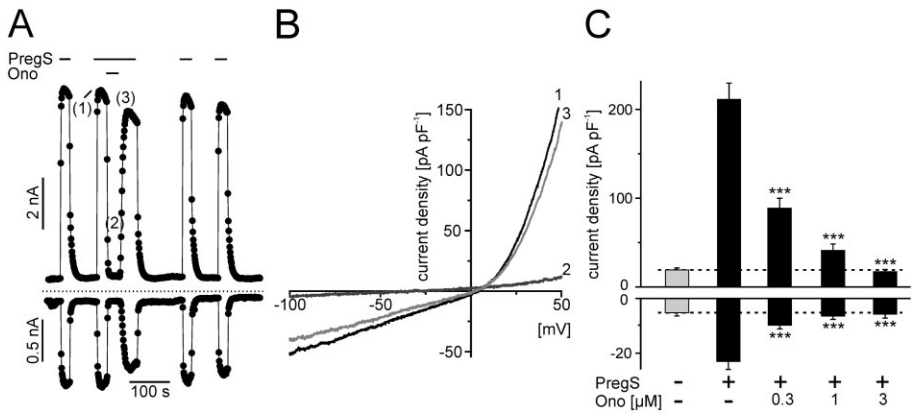

Figure 4

Electrophysiological properties of ononetin-induced TRPM3 block. (A) Whole-cell recording from a HEK_{mTRPM3} cell during stimulation with 35 μM PregS and acute addition of 3 μM ononetin. Data are extracted from voltage ramps and depict current amplitudes at 87 mV (upper trace) and –113 mV (lower trace); dotted line: zero current level. (B) I/V curve of PregS-activated TRPM3 currents before (1), during (2) and after (3) addition of 3 μM ononetin. (C) Statistical analysis of peak current densities in resting HEK_{mTRPM3} cells after addition of 35 μM PregS and different concentrations of ononetin. Data represent means and SEM of at least 11–16 independent experiments.

the TRPA1 activation in electrophysiological experiments. Whole-cell measurement of TRPA1 currents did not show significant current increases after challenging the cells with ononetin at concentrations up to 30 μM (Figure S4A). We further tested if the activation of TRPA1 by ononetin involves oxidative intermediates. Indeed, $[Ca^{2+}]_i$ responses in TRPA1 cells stimulated with low ononetin concentrations (6.25 μM) were strongly attenuated in the presence of the reducing agent DTT (10 mM, applied to the bath solution; Figure S4C–E). At higher ononetin concentrations of 12.5–25 μM, DTT exerted a lower or no inhibitory activity. By contrast, DTT supplementation did not attenuate the block of TRPM3 by ononetin. We conclude that oxidative intermediates of ononetin may be involved in activating TRPA1, but not in the block of TRPM3 by ononetin.

Next, we tested if the TRPM3-blocking compounds interfere with the endogenously expressed TRPM7 in HEK293 cells. Since external divalent cations are permanent blockers of TRPM7, switching to a bath solution lacking Ca^{2+} and Mg^{2+} gives rise to large inward currents (Nadler *et al.*, 2001). Neither TRPM7-dependent inward nor outward currents were influenced by ononetin, hesperetin or eriodictyol (20 μM each; Figure S5A). Naringenin partially blocked TRPM7 currents at a concentration of 20 μM (see Figure S5A,B).

Efficiency of naringenin and ononetin to block endogenous TRPM3 channels in isolated DRG neurones

We used mouse DRG neurones to investigate the influence of naringenin and ononetin on endogenously expressed TRPM3. Neither ononetin nor naringenin (5 μM each) had an influence on DRG neurones without a previous activation of TRPM3 by PregS (Figure 10A,D), whereas PregS-induced calcium entry was blocked by naringenin as well as ononetin (Figure 10B,E). The block of ononetin and naringenin on endogenously expressed TRPM3 was reversible, according to the measurements in HEK_{mTRPM3} cells. A significant fraction of calcium entry reappeared upon removal of naringenin or ononetin in the continuous presence of PregS (Figure 10B,E).

Next, we investigated if flavonoids are able to block TRPM3 that is endogenously expressed in rat DRG neurones. First, we detected mRNA of TRPM3 in freshly isolated rat DRG neurones via RT-PCR (data not shown). Single cell $[Ca^{2+}]_i$ measurements revealed PregS-inducible, TRPM3-like signals that were blocked by naringenin (data not shown) or ononetin (Figure 11A). Of note, the KCl-triggered activation of voltage-gated Ca^{2+} channels, identifying neuronal cells in the cultures, was not significantly affected by eriodictyol, naringenin and ononetin, reaching steady-state $[Ca^{2+}]_i$ concentrations of 698 ± 45 nM (n = 10), 626 ± 130 nM (n = 6) and 700 ± 76 nM (n = 6) respectively. We further showed that eriodictyol blocked PregS-induced calcium entry in rat DRG neurones (Figure 11B). From 165 measured DRG neurones, 90 responded to PregS of which 39 also showed a response to 2 μM capsaicin. These data indicate that rat DRG neurones also functionally express Ca^{2+}-permeable TRPM3 isoforms.

Eriodictyol has been proposed as a blocker of TRPV1 with antioxidant activity (Rossato *et al.*, 2011). In our hands, eriodictyol neither blocked capsaicin induced calcium entry in HEK293 cells stably expressing rat TRPV1 (Figure 9D) nor in freshly isolated rat DRG neurones (Figure 11B). Overall, 114 of 165 DRG neurones (69%) were still sensitive to capsaicin, although the neurones were treated with 20 μM eriodictyol. To specify the influence of eriodictyol on TRPV1, we performed whole-cell measurements of freshly isolated rat DRG neurones. Capsaicin-induced inward currents in DRG neurones were not diminished after perfusion with 20 μM eriodictyol (Figure 11C).

Discussion

In this study, we identified citrus fruit flavanone aglycones as potent and selective TRPM3 channel blockers. With IC_{50} values in the upper nanomolar (naringenin and ononetin) or low micromolar range (hesperetin and eriodictyol), these natural compounds completely and reversibly abrogate Ca^{2+}

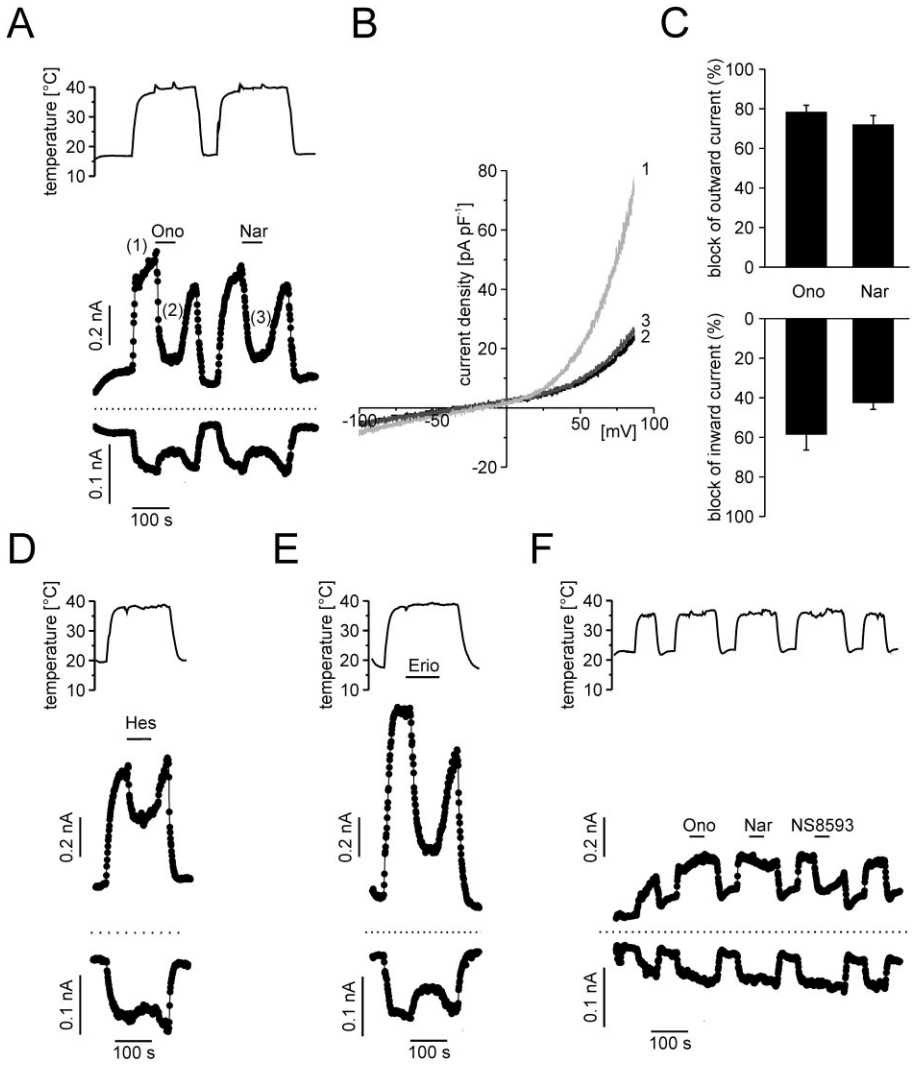

Figure 5

Heat-induced TRPM3 currents were partially blocked by TRPM3 blocker, whereas currents in non-transfected HEK293 cells were not affected by TRPM3-blocking compounds. (A) Representative whole-cell recording from a HEK293 cell transiently transfected with TRPM3α2. Elevation of the temperature of the bath solution elicited outward and inward currents (measured at 87 and –113 mV, respectively) that could be partially blocked by ononetin (10 μM) and naringenin (10 μM). (B) I/V curve of heat-activated (about 38°C) TRPM3 currents before (2) and during superfusion with 10 μM ononetin (3) or naringenin (4). (C) Aggregated data of five to six independent measurements. (D,E) Representative whole-cell measurements performed as shown in panel A, but with 10 μM hesperetin (D) or 20 μM eriodictyol (E). (F) Control experiments in non-transfected parental HEK293 cells reveal that heat-activated background currents are unaffected by superfusion with either naringenin or ononetin (10 μM each). In the presence of NS8593 (30 μM), a blocker of small conductance K^+ channels (SK1-SK3) and TRPM7 channels, heat-activated outward currents were partially inhibited.

entry and ionic currents through recombinantly expressed TRPM3α2 and block the pregnenolone sulphate-inducible Ca^{2+} entry in primary cultures of mouse or rat DRG neurones, indicating biological activity towards endogenously expressed TRPM3.

Sensory TRP channels are influenced by a large and still growing number of natural compounds, thereby mediating thermal, gustatory, odorant or eventually painful sensations (Vriens *et al.*, 2008). Flavonoids comprise the most common group of plant-derived polyphenolic compounds in the human diet. Flavanones, like naringenin and hesperetin, are a class of polyphenols that is almost exclusively contained in citrus fruits. Epidemiological and animal studies point to a possible biological activity of citrus flavonoids that might be advantageous in diseased states, such as cardiovascular disorders or cancer (for review see Benavente-Garcia and Castillo, 2008). In contrast to agonistic compounds that mimic the sensory quality of the respective TRP channel, such as a burning sensation induced by capsaicin via TRPV1 activation, chemically defined blockers do not interfere with the channel activity in the absence of an activator. Thus, it is not unexpected that, thus far, no specific sensation has been linked to the TRPM3-blocking agents. The characteristic taste of naringin or hesperidin is restricted to the respective glycoside

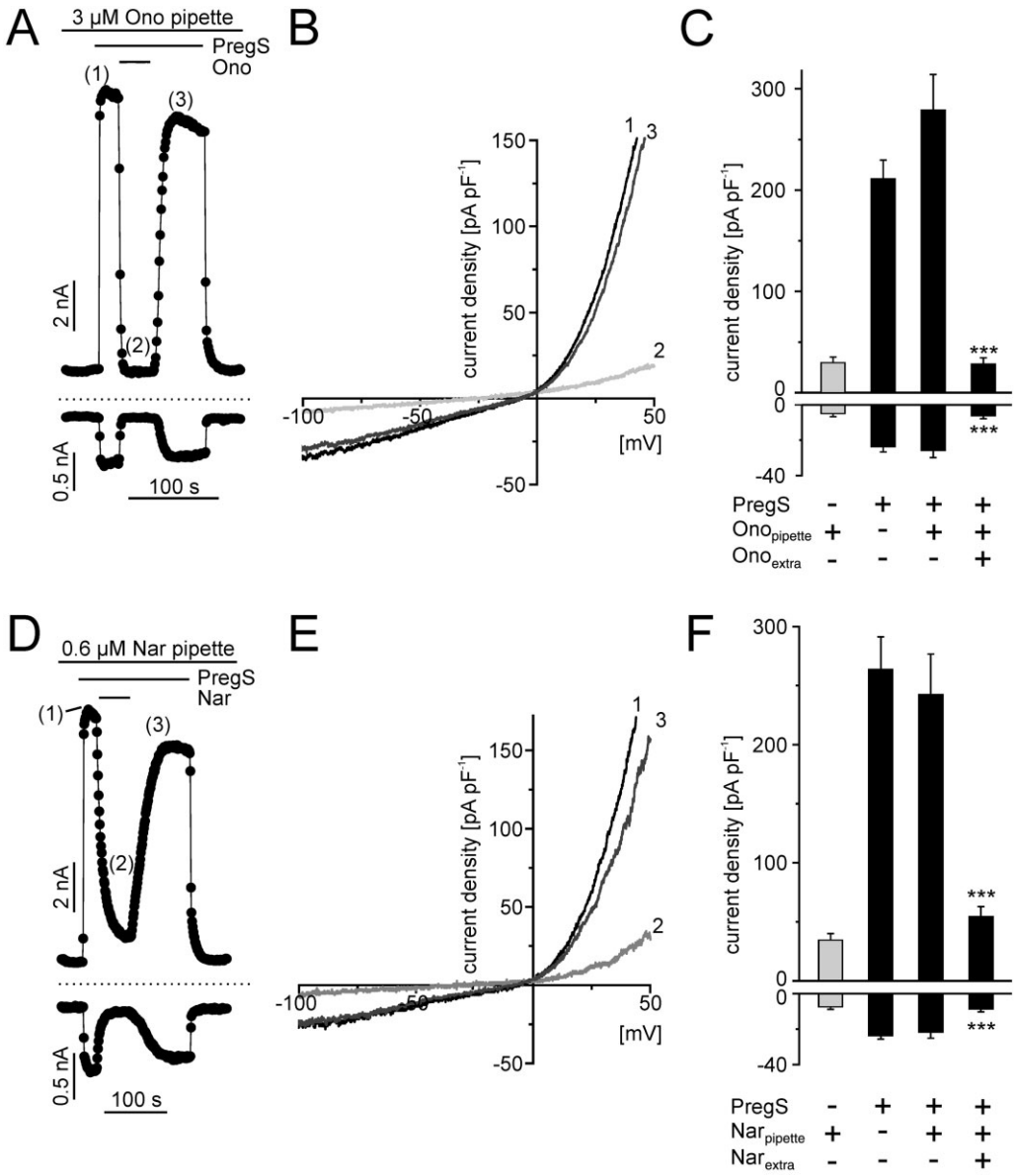

Figure 6

Binding site of naringenin and ononetin is accessible from the extracellular side. (A) and (D), representative whole-cell recording from a HEK_{mTRPM3} cell internally perfused with 3 µM ononetin (A) or 0.6 µM naringenin (D). An additional extracellular application of 35 µM PregS is still able to activate TRPM3 induced currents, which were reversibly blocked by 1 µM ononetin (A) or 1 µM naringenin (D) when added to the bath solution in the continued presence of PregS. Data are extracted from voltage ramps and depict the current at 87 mV (upper trace) and –100 mV (lower trace). Dashed lines: zero current level. Slow voltage ramps (1 mV·ms^{-1}) were applied, in the presence of 3 µM ononetin (B) or 0.6 µM naringenin (E) in the pipette, to PregS-stimulated HEK_{mTRPM3} before (1), during (2) and after (3) extracellular perfusion with 1 µM ononetin (B) or 1 µM naringenin (E). (C and F) Statistical analysis of experiments indicated in panel A or D. Data represent mean values and SEM of at least seven independent experiments for panels A–C and six independent experiments for panels D and E.

forms, but absent in the cognate TRPM3-blocking aglycones, thereby ruling out that TRPM3 is involved in sensing the bitter taste of grapefruit.

In the intestine, the flavanone glycosides hesperidin and naringin are deglycosylated to the membrane-permeable aglycones, and are then absorbed (Felgines *et al.*, 2000). Specifically, the rutinose or neohesperidose moieties are rapidly hydrolysed by enzymes of bacterial origin, such as α-rhamnosidase and β-glucosidases (Fuhr and Kummert, 1995). Considering that the glycosides did not exhibit TRPM3-blocking properties, the intestinal processing to their cognate aglycones represents a bioactivation pathway.

Until recently, naringenin has been thought to cause food-drug interactions by inhibiting cytochrome P450 enzymes. However, *in vitro* studies have shown that naringin and naringenin attenuate CYP3A4 activity by about 50% only when applied at concentrations of 200 µM (Bailey *et al.*, 2000). Meanwhile, the inhibitory effect of grapefruit juice on

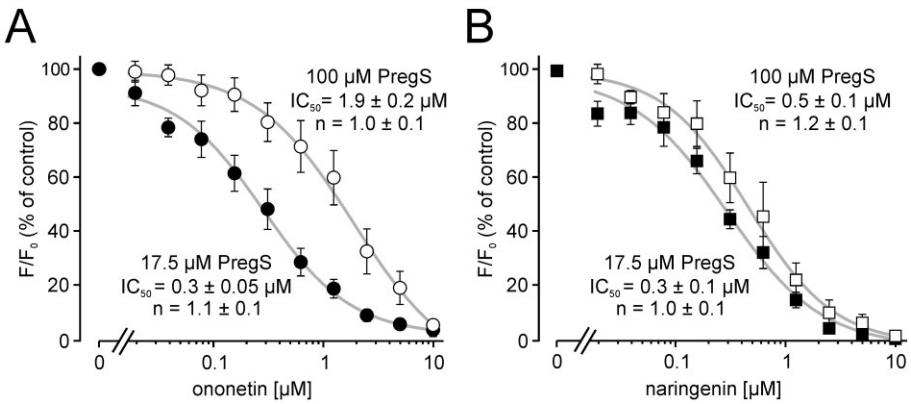

Figure 7

Naringenin and ononetin show different blocking behaviour. A HEK_{mTRPM3} cell suspension was loaded with Fluo-4 and exposed to different concentrations of ononetin (A) and naringenin (B). Calcium entry was stimulated with two different concentrations of PregS to obtain concentration–response curves. (A) Concentration–response curves of ononetin in the presence of 17.5 µM PregS and in the presence of 100 µM PregS. (B) Concentration–response curves of naringenin-induced TRPM3 channel block in the presence of 17.5 µM PregS and in the presence of 100 µM PregS. Shown are means and SEM of at least three to five different experiments in duplicates each. IC_{50} values and Hill coefficients (*n*) were obtained by non-linear curve fitting, applying a four-parameter Hill plot.

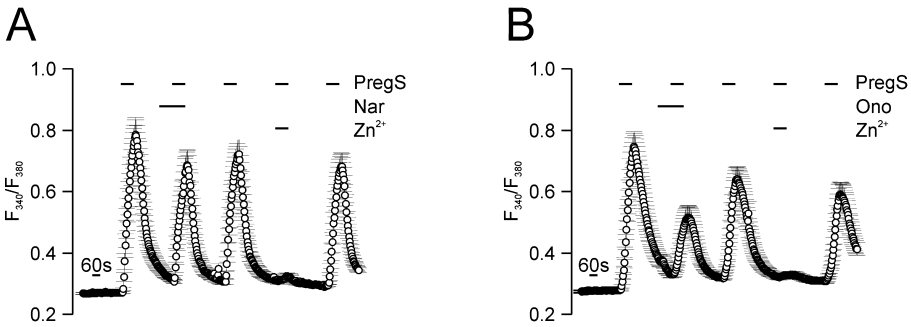

Figure 8

Naringenin affects Ca^{2+} entry through TRPM1only weakly and ononetin partially blocks TRPM1 channels. Single cell calcium imaging experiments with HEK293 cells transiently transfected with cDNA plasmids encoding TRPM1 and loaded with the fluorometric Ca^{2+} indicator fura 2. TRPM1 was activated with 50 µM PregS alone and in the presence of 10 µM naringenin (n = 44) (A) or 10 µM ononetin (n = 50) (B), followed by application of PregS alone and in combination with 100 µM $ZnCl_2$. Shown are means and SEM of at least four to six independent imaging experiments.

CYP3A4 has been attributed to more potently inhibiting constituents, such as the furanocoumarins bergamottin and bergapten (Hanley *et al.*, 2011). Nonetheless, naringenin and hesperetin are substrates of CYP-mediated hydroxylation, resulting in the formation of the common metabolite eriodictyol. Since both the CYP substrates as well as their product display a similar IC_{50}, and since the kinetics of the block is fast and reversible, we conclude that the biological activity to block TRPM3 is neither related to CYP activity, nor to its inhibition.

With an IC_{50} of 0.5 µM, naringenin is the most potent TRPM3-blocking flavanone. The additional hydroxyl group at the C3′ atom found in hesperetin and eriodictyol diminishes the potency of the TRPM3 block to low micromolar concentrations. Despite a slightly lower potency, however, the C3′ hydroxylation increased the selectivity for TRPM3. Neither eriodictyol nor hesperetin discernibly influenced the sensory TRP ion channels TRPV1, TRPM8, TRPA1. By contrast, higher concentrations of naringenin modulated HEK293 cells stably expressing TRPM8 in a complex fashion that was reminiscent of a partial agonism, followed by deactivation of TRPM8.

With respect to TRPM1, the closest relative of TRPM3, we found that 10 µM ononetin, but not naringenin inhibited PregS-induced $[Ca^{2+}]_i$ signals that are mediated by TRPM1 by about 50%. Considering that the IC_{50} of ononetin to block TRPM3 is 0.3 µM, the selectivity of ononetin is still 30-fold and can be employed to differentiate between these channels. With an IC_{50} of 300 nM, the deoxybenzoin ononetin is, to our knowledge, the most potent TRPM3 blocker that has been identified so far. Ononetin is a still poorly characterized compound. Ononetin and other deoxybenzoins have been shown to confer antioxidant properties and, at concentrations above 10 µM, to inhibit tyrosinases (Ng *et al.*, 2009). Since the ononetin-induced activation of TRPA1 is partially sensitive to

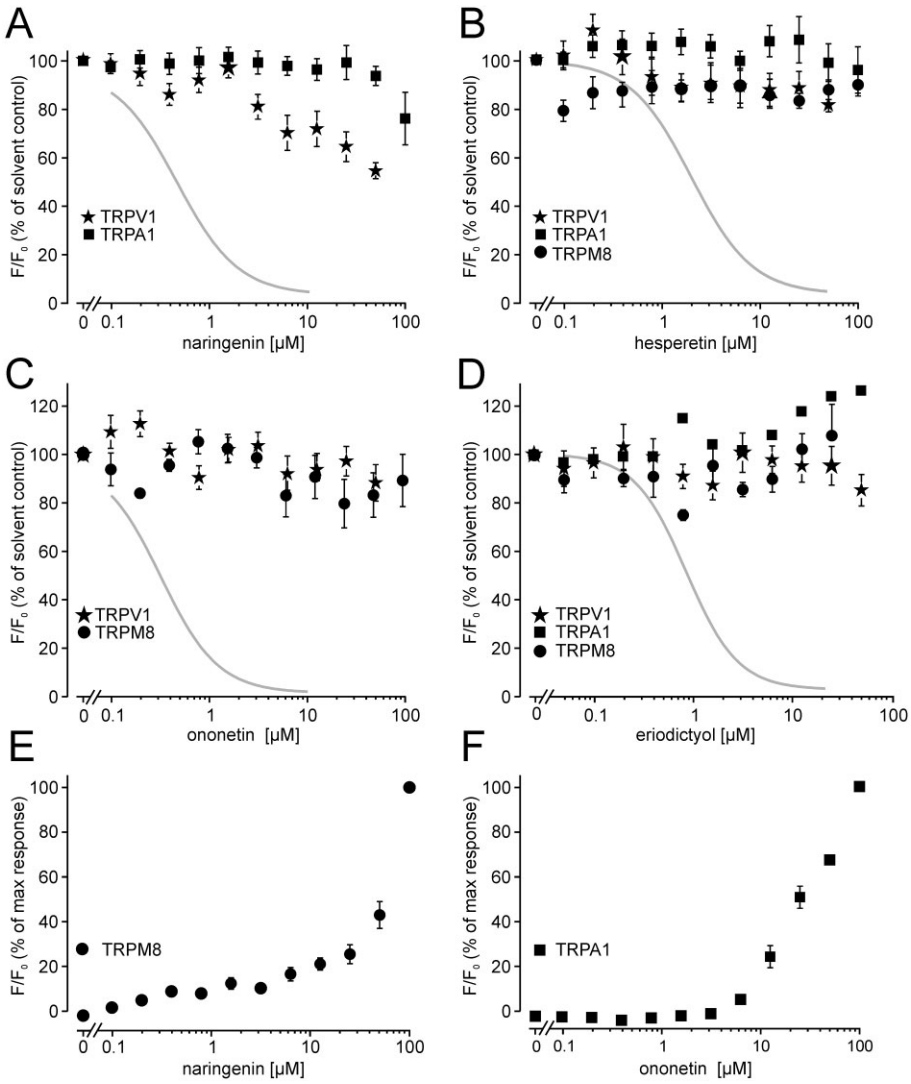

Figure 9

Effects of TRPM3 channel blockers on other sensory TRP channels. HEK293 cells stably expressing the indicated TRP channels were preincubated with naringenin (A), hesperetin (B), ononetin (C) or eriodictyol (D); and activation of the respective channels was followed by measuring increases in the fluorescence intensity of intracellularly loaded Fluo-4, or in $HEK_{rTRPV1:YFP}$ cells, by monitoring the Ca^{2+} influx-mediated intracellular acidification, causing a decrease in the fluorescence intensity of co-expressed YFP (Hellwig *et al.*, 2004). The respective activators are 2 μM capsaicin for TRPV1, 30 μM AITC for TRPA1 and 300 μM menthol for TRPM8. Data represent mean and SEM of three to six different experiments, performed in duplicate each. Grey curves indicate the Hill fit of TRPM3 block by the indicated compounds. (E) Naringenin-induced Ca^{2+} entry in $HEK_{hTRPM8:CFP}$ and (F) ononetin-induced calcium entry in HEK_{hTRPA1} cells.

the reducing agent DTT, oxidated ononetin intermediates may be involved. The block of TRPM3, however, requires very low ononetin concentrations, develops within a few seconds and is not counteracted by 10 mM DTT, arguing against a necessity of oxidation for TRPM3 block. Ononetin can be produced from the isoflavone ononin (Hlasiwetz, 1855), an isoflavone glycoside that is not only found in the name-giving plant *O. spinosa* but also contained in edible plants, such as soy bean and clover. Owing to their structural similarity to estradiol and transactivation of the estrogen receptors ERα and ERβ, isoflavones are regarded as phytoestrogens (Cederroth and Nef, 2009). A structural relationship between ononetin and steroids may provide the structural basis of a competitive interference between ononetin and the neurosteroid PregS with regard to TRPM3 binding. Indeed, the blocker sensitivity was attenuated when exposing TRPM3 to higher PregS concentrations (see Figure 7). However, both competitive binding to the activator site or allosteric modulation that mutually impedes on the ligand-binding properties may explain these effects.

Of note, the TRPM3 gene transcripts are spliced into several splice variants that either bear a Ca^{2+}-permeable pore (e.g. the α2 variant) or to an α1 variant whose pore is selective for monovalent cations and not activated by PregS (Oberwinkler *et al.*, 2005). Since activators of the α1 variant are still unknown, and since fluorometric Ca^{2+} assays are inapplicable

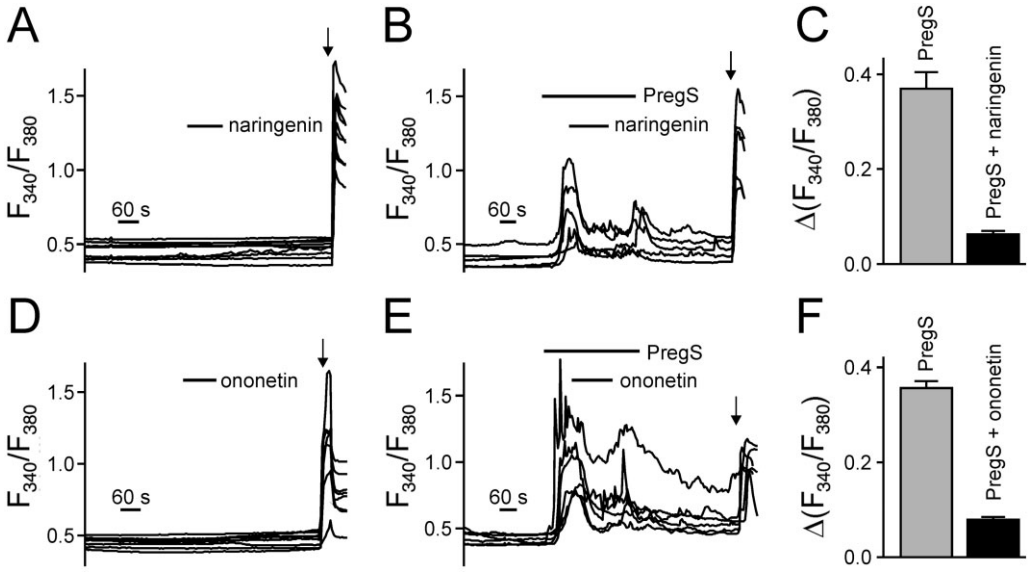

Figure 10

PregS-evoked Ca^{2+} influx in mouse DRG neurones is reduced by naringenin or ononetin. (A,B) Example traces of single DRG neurones in calcium imaging measurements. Freshly dissociated DRG neurones were loaded with Fura-2/AM, and fluorescence changes at 340 and 380 nm were measured. DRG neurones were superfused with 5 μM naringenin alone (A) or simultaneously with 50 μM PregS that was applied longer than the inhibitor (B). (C) Statistical analysis of data similar to those presented in (B). A total number of 70 DRG neurones were monitored in nine microfluorometric imaging experiments to obtain these data. (D,E) Sample traces of single DRG neurones similar to panel A except 5 μM of ononetin was applied alone (D) or simultaneously with PregS (applied longer than ononetin) (E). (F) Statistical analysis of experiments performed in panel E. A total number of 163 neurones were analysed in eight imaging experiments. Bath solutions contained (20 μM) verapamil to suppress voltage-gated calcium channel activity. Intact neurones were identified at the end of the experiment by applying 75 mM KCl in the absence of verapamil (indicated by arrows).

with this isoform, we did not assess the effects of ononetin or flavanones on TRPM3α1. In addition, fluorometric assays in DRG neurones relied on a PregS-triggered Ca^{2+} entry and, thus, most likely reflect splice variants that share the α2 pore conformation.

Since naringenin and ononetin also blocked the TRPM3 activation by nifedipine, an activator that is chemically unrelated to PregS, a competitive mode of action appears unlikely. In addition, heat-mediated TRPM3 activation is also strongly blocked by both compounds. Thus, naringenin and ononetin induced block is not restricted to PregS activation of TRPM3. In this study, we provide evidence for a binding mode that involves the extracellularly accessible moieties of the channel protein and exhibits a slight voltage dependence in favour of blocking the physiologically more relevant inward current component and a reversible mode of action. A more thorough electrophysiological characterization, including a detailed kinetic analysis, the assessment of use dependence, and profiling of single channel properties in the presence of the blockers, may provide additional insights in the mechanism of TRPM3 block by these natural compounds.

Another still unresolved question relates to the localization of the binding site of the flavanones and deoxybenzoins on TRPM3. Electrophysiological data obtained with intracellularly perfused modulators demonstrated that TRPM3 was still activated by PregS, and that the same modulator only blocked this conductance when added to the bath solution. Although the most common interpretation would be that the binding site is accessible from the extracellular space, the unrestricted membrane permeability of the aglycones may result in a rapid intracellular dilution of the TRPM3 modulator. In addition, the insensitivity of TRPM3 to the glycosides is likely to result from an inability of flavanone glycosides to bind to TRPM3. An alternative explanation could be that the more hydrophilic compound is largely membrane-impermeable and might not reach an intracellular binding site on TRPM3. Thus, more detailed analyses of the modulator-binding properties and on the interference with the channel gating will be addressed in future by electrophysiological studies.

TRPM3 is expressed in nociceptive sensory neurones in dorsal root and trigeminal ganglia, and its activation has been linked to thermal pain. Specifically, $TRPM3^{-/-}$ mice show an attenuated response to thermal nociceptive stimuli, an effect that is maintained after induction of inflammatory hyperalgesia (Vriens *et al.*, 2011). Here we show that naringenin as well as ononetin block the PregS-induced Ca^{2+} entry in freshly isolated neurones from mouse DRG. Besides DRG neurones from mice, TRPM3-like responses were also found in PregS-stimulated freshly isolated rat DRG neurones, and these responses were blocked by eriodictyol. Rossato *et al.* (2011) showed that eriodictyol is a potent blocker of TRPV1 with analgesic effects on capsaicin-treated mice and complete Freund's adjuvant-induced thermal hyperalgesia. Astonishingly, and in contrast to this report, we observed that eriodictyol is

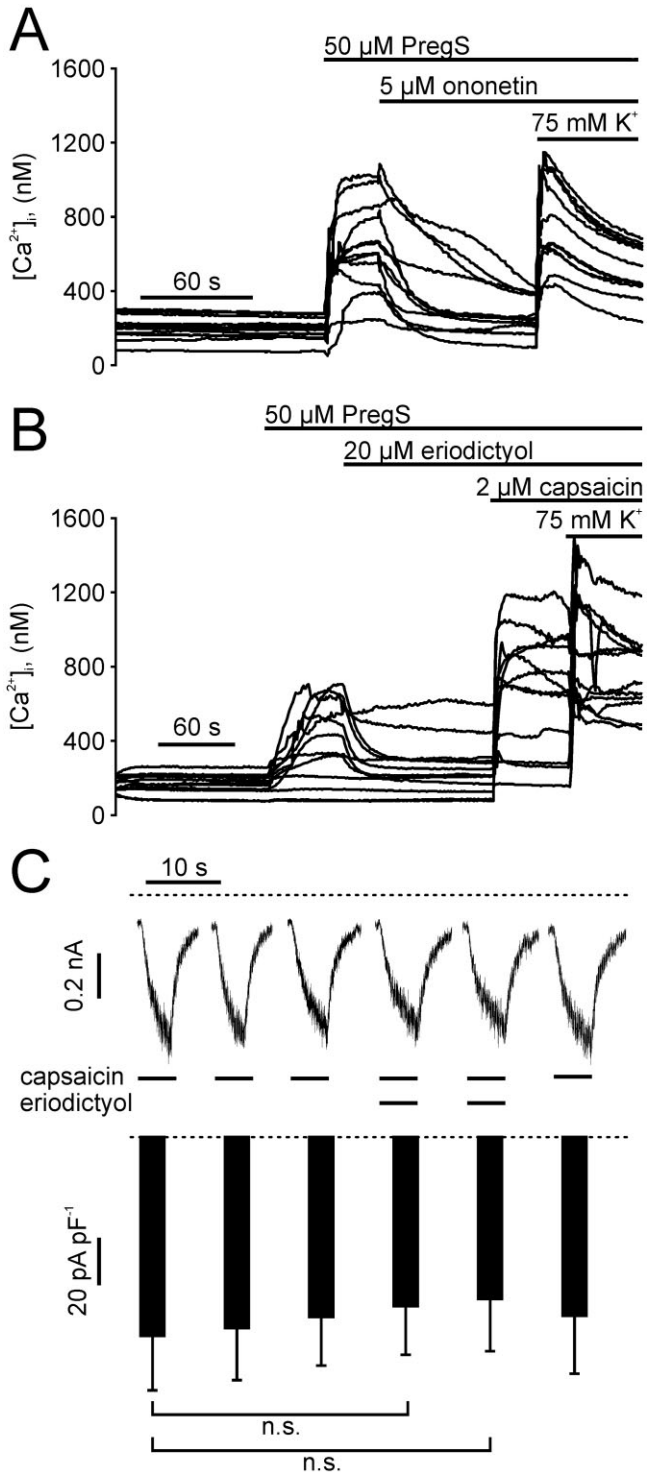

Figure 11

Eriodictyol blocks TRPM3, but not TRPV1 in rat DRG neurones. (A) Sample traces of intracellular calcium concentration in single rat DRG neurones during addition of 50 µM PregS, 5 µM ononetin and 75 mM KCl. (B) Similar experiment as in (A), but with addition of 20 µM eriodictyol and 2 µM capsaicin. (C). Upper panel: Whole-cell currents in a freshly isolated rat DRG neuron voltage-clamped at −70 mV. Capsaicin (1 µM) alone, or in combination with eriodictyol (20 µM) was applied for 5 s intervals. Lower panel: Statistical analysis of 8 independent measurements (means and SEM) performed as shown in the upper panel. n.s., statistically not significant.

a potent blocker of TRPM3, but not of TRPV1. The inability of eriodictyol to block the capsaicin-induced activation of rat TRPV1 was tested in a recombinant expression system and confirmed in freshly isolated rat DRG neurones. Since we cannot confirm the TRPV1-blocking properties of eriodictyol, one should consider the possibility that the thermal hypoalgesia that has been observed by Rossato *et al*. may be related to the block of TRPM3.

Due to the availability of pharmacokinetic and toxicological data, flavanones such as naringenin may be applied *in vitro* as well as *in vivo* studies. In mice, naringenin has an LD_{50} of more than 5 $g \cdot kg^{-1}$ (Ortiz-Andrade *et al*., 2008). Therefore, a potential antinociceptive effect of citrus fruit flavanones may be tested *in vivo* and might reveal a therapeutic potential for analgesic treatment.

After consumption of grapefruit juice and orange juice, plasma concentrations of naringenin and hesperetin may reach low micromolar concentrations (Erlund *et al*., 2001). Once resorbed, they undergo extensive phase 1 and phase 2 metabolization via hydroxylation, glucuronidation and sulfatation (Fuhr and Kummert, 1995). Thus, if citrus fruit flavonoids exert promising pharmacodynamic properties, a further compound optimization should be considered to avoid a rapid modification. Alternatively, the modulators might be applied topically, or the bioavailability and stability of naringenin may be enhanced by complexation with hydroxyl-β-cyclodextrin (Shulman *et al*., 2011).

In summary, we identified specific and potent blockers of TRPM3 that can be used to investigate its function *in vivo* and *in vitro*. Since the physiological functions of TRPM3 are still not firmly established, we expect that acute TRPM3 modulation with pharmacological modulators provides a useful and validated cell-biological tool to study TRPM3 *in vitro* and *in vivo* and to complement transgenic approaches. Furthermore, if the involvement of TRPM3 in nociception could be strengthened, TRPM3-blockers may offer a novel mode of action for analgesic treatment.

Acknowledgements

This work was supported by the Deutsche Forschungsgemeinschaft within the frameworks of FOR 806 and the GK 1097 to MS, the Emmy Noether-programme, GK 1326, SFB 593 and SFB 894 to JO, and the GK1326 and SFB 894 to SEP. We thank Helga Sobottka, Marion Leonhardt, Sandra Plant and Raissa Wehmeyer for excellent technical support.

Conflicts of interest

The authors state no conflict of interest.

References

Abramoff MD, Magalhaes PJ, Ram SJ (2004). Image processing with ImageJ. Biophotonics Int 11: 36–42.

Bailey DG, Dresser GK, Kreeft JH, Munoz C, Freeman DJ, Bend JR (2000). Grapefruit-felodipine interaction: effect of unprocessed fruit and probable active ingredients[ast]. Clin Pharmacol Ther 68: 468–477.

Benavente-Garcia O, Castillo J (2008). Update on uses and properties of citrus flavonoids: new findings in anticancer, cardiovascular, and anti-inflammatory activity. J Agric Food Chem 56: 6185–6205.

Breinholt VM, Offord EA, Brouwer C, Nielsen SE, Brosen K, Friedberg T (2002). In vitro investigation of cytochrome P450-mediated metabolism of dietary flavonoids. Food Chem Toxicol 40: 609–616.

Cederroth CR, Nef S (2009). Soy, phytoestrogens and metabolism: a review. Mol Cell Endocrinol 304: 30–42.

Edelstein A, Amodaj N, Hoover K, Vale R, Stuurman N (2010). Computer Control of Microscopes Using -μManager. Curr Protoc Mol Biol 92: 14.20.1–14.20.17.

Erlund I, Meririnne E, Alfthan G, Aro A (2001). Plasma kinetics and urinary excretion of the flavanones naringenin and hesperetin in humans after ingestion of orange juice and grapefruit juice. J Nutr 131: 235–241.

Felgines C, Texier O, Morand C, Manach C, Scalbert A, Régerat F *et al.* (2000). Bioavailability of the flavanone naringenin and its glycosides in rats. Am J Physiol Gastrointest Liver Physiol 279: G1148–G1154.

Fuhr U, Kummert AL (1995). The fate of naringin in humans: a key to grapefruit juice-drug interactions? Clin Pharmacol Ther 58: 365–373.

Grimm C, Kraft R, Schultz G, Harteneck C (2005). Activation of the melastatin-related cation channel TRPM3 by D-erythro-sphingosine [corrected]. Mol Pharmacol 67: 798–805.

Hanley MJ, Cancalon P, Widmer WW, Greenblatt DJ (2011). The effect of grapefruit juice on drug disposition. Expert Opin Drug Metab Toxicol 7: 267–286.

Harteneck C, Schultz G (2007). TRPV4 and TRPM3 as volume-regulated cation channels. In: Liedtke WB, Heller S (eds). TRP Ion Channel Function in Sensory Transduction and Cellular Signaling Cascades. CRC Press: Boca Raton, FL.

Hellwig N, Plant TD, Janson W, Schafer M, Schultz G, Schaefer M (2004). TRPV1 acts as proton channel to induce acidification in nociceptive neurons. J Biol Chem 279: 34553–34561.

Hill K, Schaefer M (2009). Ultraviolet light and photosensitising agents activate TRPA1 via generation of oxidative stress. Cell Calcium 45: 155–164.

Hlasiwetz H (1855). Ueber die Wurzel der Ononis spinosa. J Prakt Chem 65: 419–450.

Kilkenny C, Browne W, Cuthill IC, Emerson M, Altman DG (2010). NC3Rs Reporting Guidelines Working Group. Br J Pharmacol 160: 1577–1579.

Klose C, Straub I, Riehle M, Ranta F, Krautwurst D, Ullrich S *et al.* (2011). Fenamates as TRP channel blockers: mefenamic acid selectively blocks TRPM3. Br J Pharmacol 162: 1757–1769.

Lambert S, Drews A, Rizun O, Wagner TF, Lis A, Mannebach S *et al.* (2011). Transient receptor potential melastatin 1 (TRPM1) is an ion-conducting plasma membrane channel inhibited by zinc ions. J Biol Chem 286: 12221–12233.

Leffler A, Fischer MJ, Rehner D, Kienel S, Kistner K, Sauer SK *et al.* (2008). The vanilloid receptor TRPV1 is activated and sensitized by local anesthetics in rodent sensory neurons. J Clin Invest 118: 763–776.

Lenz JC, Reusch HP, Albrecht N, Schultz G, Schaefer M (2002). Ca^{2+}-controlled competitive diacylglycerol binding of protein kinase C isoenzymes in living cells. J Cell Biol 159: 291–302.

Majeed Y, Bahnasi Y, Seymour VA, Wilson LA, Milligan CJ, Agarwal AK *et al.* (2011). Rapid and contrasting effects of rosiglitazone on transient receptor potential TRPM3 and TRPC5 channels. Mol Pharmacol 79: 1023–1030.

Manach C, Scalbert A, Morand C, Rémésy C, Jiménez L (2004). Polyphenols: food sources and bioavailability. Am J Clin Nutr 79: 727–747.

McGrath J, Drummond G, McLachlan E, Kilkenny C, Wainwright C (2010). Guidelines for reporting experiments involving animals: the ARRIVE guidelines. Br J Pharmacol 160: 1573–1576.

Nadler MJS, Hermosura MC, Inabe K, Perraud AL, Zhu Q, Stokes AJ *et al.* (2001). LTRPC7 is a MgATP-regulated divalent cation channel required for cell viability. Nature 411: 590–595.

Naylor J, Li J, Milligan CJ, Zeng F, Sukumar P, Hou B *et al.* (2010). Pregnenolone sulphate- and cholesterol-regulated TRPM3 channels coupled to vascular smooth muscle secretion and contraction. Circ Res 106: 1507–1515.

Ng LT, Ko HH, Lu TM (2009). Potential antioxidants and tyrosinase inhibitors from synthetic polyphenolic deoxybenzoins. Bioorg Med Chem 17: 4360–4366.

Norenberg W, Hempel C, Urban N, Sobottka H, Illes P, Schaefer M (2011). Clemastine potentiates the human P2X7 receptor by sensitizing it to lower ATP concentrations. J Biol Chem 286: 11067–11081.

Oberwinkler J, Lis A, Giehl KM, Flockerzi V, Philipp SE (2005). Alternative splicing switches the divalent cation selectivity of TRPM3 channels. J Biol Chem 280: 22540–22548.

Ortiz-Andrade RR, Sánchez-Salgado JC, Navarrete-Vázquez G, Webster SP, Binnie M, García-Jiménez S *et al.* (2008). Antidiabetic and toxicological evaluations of naringenin in normoglycaemic and NIDDM rat models and its implications on extra-pancreatic glucose regulation. Diabetes Obes Metab 10: 1097–1104.

Rossato MF, Trevisan G, Walker CI, Klafke JZ, de Oliveira AP, Villarinho JG *et al.* (2011). Eriodictyol: a flavonoid antagonist of the TRPV1 receptor with antioxidant activity. Biochem Pharmacol 81: 544–551.

Shulman M, Cohen M, Soto-Gutierrez A, Yagi H, Wang H, Goldwasser J *et al.* (2011). Enhancement of naringenin bioavailability by complexation with hydroxypropoyl-β-cyclodextrin. PLoS ONE 6: e18033.

Urban N, Hill K, Wang L, Kuebler WM, Schaefer M (2012). Novel pharmacological TRPC inhibitors block hypoxia-induced vasoconstriction. Cell Calcium 51: 194–206.

Vriens J, Nilius B, Vennekens R (2008). Herbal compounds and toxins modulating TRP channels. Curr Neuropharmacol 6: 79–96.

Vriens J, Owsianik G, Hofmann T, Philipp SE, Stab J, Chen X *et al.* (2011). TRPM3 is a nociceptor channel involved in the detection of noxious heat. Neuron 70: 482–494.

Wagner TF, Loch S, Lambert S, Straub I, Mannebach S, Mathar I *et al.* (2008). Transient receptor potential M3 channels are ionotropic steroid receptors in pancreatic beta cells. Nat Cell Biol 10: 1421–1430.

Wagner TF, Drews A, Loch S, Mohr F, Philipp SE, Lambert S *et al.* (2010). TRPM3 channels provide a regulated influx pathway for zinc in pancreatic beta cells. Pflugers Arch 460: 755–765.

Xu SZ, Zeng F, Boulay G, Grimm C, Harteneck C, Beech DJ (2005). Block of TRPC5 channels by 2-aminoethoxydiphenyl borate: a differential, extracellular and voltage-dependent effect. Br J Pharmacol 145: 405–414.

Zamudio-Bulcock PA, Everett J, Harteneck C, Valenzuela CF (2011). Activation of steroid-sensitive TRPM3 channels potentiates glutamatergic transmission at cerebellar Purkinje neurons from developing rats. J Neurochem 119: 474–485.

Supporting information

Additional Supporting Information may be found in the online version of this article at the publisher's web-site:

Figure S1 Concentration–response curves of naringenin-induced TRPM3 block. Whole-cell recordings of HEK_{mTRPM3} cells stimulated with 35 μM of PregS and blocked with different concentration of naringenin were performed to obtain concentration–response curves. To avoid that the rundown of the channel is considered as block, an interpolated value between before and after block was used to calculate the percent of block. A time-matched activation of TRPM3 without naringenin was set as 100%, and measurements in the presence of naringenin were normalized to this value. (A) Representative recordings of whole-cell currents. Data are extracted from voltage ramps and depict the current at 87 mV (upper trace) and −113 mV (lower trace). Dotted line: zero current level. (B–C) Concentration–response curves of naringenin to block PregS-induced inward currents (B) and outward currents (C). IC_{50} values and Hill coefficients (*n*) were obtained by non-linear curve fitting, applying a four-parameter Hill equation. Each data point represents SEM of 5–12 independent experiments.

Figure S2 Naringenin and ononetin block nifedipine-induced TRPM3 currents in HEK_{mTRPM3} cells. (A) Whole-cell recording from a HEK_{mTRPM3} cell stimulated with 50 μM nifedipine and 35 μM PregS. And further nifedipine-induced TRPM3 currents were blocked with either 1 or 3 μM of ononetin. Data are extracted from voltage ramps and depict current amplitudes at 87 mV (upper trace) and −113 mM (lower trace); dotted line: zero current level (B) IV curve of PregS- (1) and nifedipine-activated TRPM3 currents (2) and during an additional stimulation with 1 μM (3) or 3 μM ononetin (4). (C) Statistical analysis of peak current densities in resting HEK_{mTRPM3} cells after addition of 50 μM nifedipine and different concentrations of ononetin. (D–E) Similar experiments as described for panels A–C, whereas ononetin was replaced by naringenin. Data represent means and SEM of at least 5–10 independent experiments for naringenin and six independent experiments for ononetin.

Figure S3 Naringenin has activating and blocking potency in HEK293 cells stably expressing TRPM8. (A) Examples of calcium entry traces from Fluo 4-loaded HEK_{hTRPM8} cells activated with different concentrations of naringenin and menthol. Challenging the cells with naringenin concentration-dependently prevented the subsequent activation with 300 μM menthol. (B) Example of a whole-cell recording of a HEK293 cell stably expressing TRPM8. The cell was either perfused with 100 μM naringenin alone, simultaneously with 300 μM menthol or after an activation of TRPM8 with 300 μM menthol. Note the partial activation of outward currents and the block of menthol-induced currents in the presence of naringenin.

Figure S4 Ononetin does not activate TRPA1 in whole-cell patch clamp measurements, but it activates DTT-dependent TRPA1 in fluorometric measurements. (A–B) Representative whole-cell recordings from HEK293 cells stably expressing TRPA1. Cells were first perfused with 10 μM (A) or 30 μM ononetin (B). An additional perfusion with AITC (10 μM) induced TRPA1 currents. (C–D) Examples of calcium entry traces from Fluo4-loaded HEK_{hTRPA1} cells activated with different concentrations of ononetin and 30 μM of AITC (C) and in the presence of 10 mM of DTT (D). (E) Statistical analysis of differences in ononetin-induced calcium entry in the presence of 10 mM DTT. Calcium entry after 30 μM AITC without ononetin was set as maximal activation. Data represent means and SEM of at least three independent experiments in duplicate each. $*P < 0.05$; $**P < 0.01$

Figure S5 Endogenously expressed TRPM7 in HEK293 cells is partially blocked by naringin, whereas ononetin, hesperetin and eriodictyol did not affect TRPM7 currents. (A) Representative whole-cell recordings from HEK293 cells endogenously expressing TRPM7. Perfusion of the cells with a solution containing no divalent cations elicited linear TRPM7 currents. An additional perfusion with 20 μM ononetin, 20 μM hesperetin and 20 μM eriodictyol did not significantly influence the TRPM7 current, whereas 20 μM naringenin partially blocked the inward and outward currents. (B) Statistical analysis of percentage of block of 5–10 independent measurements. $**P < 0.01$